AQUA
Water Infrastructure, Ecosystems and Society

IWA PUBLISHING

 AQUA — Water Infrastructure, Ecosystems and Society Vol 70 No 8, 1159 doi: 10.2166/aqua.2021.026

Degradation of 2,6-dichloro-1,4-benzoquinone by advanced oxidation with UV, H_2O_2, and O_3: parameter optimization and model building

Zhangbin Pan[a,b], Xiaokang Zhu[b,c], Guifang Li[b], Yongqiang Wang[b,c], Mei Li[c], Shaohua Sun[b], Ruibao Jia[IWA b] and Li'an Hou[a,b,d,*]

[a] College of Chemical Engineering, China University of Petroleum (East China), Qingdao 266580, China
[b] Shandong Province Water Supply and Drainage Monitoring Center, Jinan 250101, China
[c] School of Municipal & Environmental Engineering, Shandong Jianzhu University, Jinan 250101, China
[d] Xi'an High-Tech Institute, Xi'an 710025, China
*Corresponding author. E-mail: houla@cae.cn

ABSTRACT

Halobenzoquinones are disinfection by-products with cytotoxicity, carcinogenicity, and genotoxicity. In this study, we investigated the removal of the HBQ 2,6-dichloro-1,4-benzoquinone (DCBQ) from water using advanced oxidation processes. The removal of DCBQ from water using UV, H_2O_2, and O_3 advanced oxidation processes individually was not ideal with removal rates of 36.1% with a UV dose of 180 mJ/cm^2, 32.0% with 2 mg/L H_2O_2, and 57.9% with 2 mg/L O_3. Next, we investigated using the combined UV/H_2O_2/O_3 advanced oxidation process to treat water containing DCBQ. A Box–Behnken design was used to optimize the parameters of the UV/H_2O_2/O_3 process, which gave the following optimum DCBQ removal conditions: UV dose of 180 mJ/cm^2, O_3 concentration of 0.51 mg/L, and H_2O_2 concentration of 1.76 mg/L. The DCBQ removal rate under the optimum conditions was 94.3%. We also found that lower humic acid concentrations promoted DCBQ degradation, while higher humic acid concentrations inhibited DCBQ degradation.

Key words: 2,6-dichloro-1,4-benzoquinone, Box–Behnken design, degradation pathway, drinking water, halogenated benzoquinone

HIGHLIGHTS

- Box–Behnken design (BBD) was used to optimize the parameters of UV/H_2O_2/O_3 process for the degradation of 2,6-dichloro-1,4-benzoquinone (DCBQ). A secondary model was developed to eliminate DCBQ to the maximum extent.
- The combined UV/H_2O_2/O_3 process proposed in this study can be used to control the by-products of halogenated benzoquinone disinfection in water plant.

INTRODUCTION

Trace organic pollutants of natural and human origins are often detected in drinking water sources (Shimabuku *et al.* 2019). Disinfection by-products (DBPs) are produced by the reaction of dissolved organic matter in water with chlorine (Nikolaou *et al.* 2004). Because of their confirmed or potential carcinogenicity, many DBPs have received increasing attention, especially in the treatment of slightly polluted water sources.

Halobenzoquinones (HBQs) have been identified as an emerging class of DBPs. HBQs are cytotoxic and may be carcinogenic and genotoxic and cause DNA damage through oxidative stress (Wei *et al.* 2016). Water containing HBQs should be treated to protect human health. Zhao *et al.* (2010) detected HBQs in tap water from Canada and found that the compounds with the highest concentrations were 2,6-dichloro-1,4-benzoquinone (DCBQ; 165.1 ± 9.1 ng/L), 2,6-dichloro-3methyl-1,4-benzoquinone (1.3 ± 0.2 ng/L), 2,3,6-trichloro-1,4-benzoquinone (9.1 ± 0.6 ng/L), and 2,6-dibromo-1,4-benzoquinone (0.5 ± 0.1 ng/L). Zuo *et al.* (2017) evaluated the toxicity of DCBQ using *Caenorhabditis elegans*, and found that DCBQ had stronger general toxicity than controlled DBPs, and caused some inheritable genetic mutations *in vivo*.

Advanced oxidation processes remove organic pollutants from water and can greatly reduce the reaction time and make mineralization easier. Various organic pollutants can be completely decomposed in a few hours by the generated free radicals, which are strong oxidants (Chen *et al.* 2018). Ozonation is used as a treatment technology to remove pollutants from water through direct ozonation and indirect hydroxyl radical (HO•)-induced oxidation reactions. The main ozone-

based advanced oxidation processes are O_3, UV/O_3, and UV/H_2O_2/O_3. Research has shown that the DCBQ removal rate with potassium ferrate (K_2FeO_4) can be as high as 87.12%, but the reaction is greatly affected by the pH with the removal rate decreasing under alkaline conditions (Ding *et al.* 2018). Advanced oxidation technology with UV utilizes the strong oxidation property of $HO^{\cdot}$ ($E_0 = 2.80$ V) to non-selectively degrade organic pollutants (Du *et al.* 2020) in a green method with high efficiency. This method has been applied in drinking water plants around the world. In addition, as a back-end deep treatment process, this method can control HBQs generated in the process of containing or pre-oxidizing raw water. Further research on the degradation of HBQs by UV advanced oxidation process is required.

The controlled variable method requires a large number of experiments to determine the optimum level for a variable and cannot reflect the comprehensive effect of various factors. Response surface methodology (RSM) can jointly optimize all parameters and overcome the limitations of the controlled variable method (Elibol 2002). RSM can be used to determine the optimum conditions for a multivariable system. It is a collection of mathematical and statistical techniques that can be used to develop, improve, and optimize processes. Using RSM, we can evaluate the relationship between experimental factors and measured responses and the relative influence of factors. The main goal of RSM is to determine the optimum operating conditions of a system to meet the operating specifications. In RSM designs, low-, medium-, and high-level codes are usually expressed as -1, 0, and $+1$, respectively. In different experiments, the levels of one factor are combined with the levels of other factors. A mathematical model of the relationship between the response value and each factor is generated from the results of the optimization experiments (Schenone *et al.* 2015).

In this study, DCBQ, which has the highest detection frequency and highest concentrations in water among the HBQs, was selected as the target pollutant. The suitability of the UV/H_2O_2/O_3 process for the removal of DCBQ was evaluated. The main purpose of this study was to study the effects of O_3, H_2O_2, and UV on DCBQ removal. A Box–Behnken design (BBD) was used to study the effects of the UV dose, H_2O_2 concentration, and O_3 concentration on their own and in interaction, and a quadratic model was developed for DCBQ removal. The influence of natural organic matter (NOM) on the UV/H_2O_2/O_3 degradation pathway was also explored.

METHODS

Materials

Formic acid and methanol (chromatography grade) were used in this study. DCBQ was purchased from Sigma–Aldrich (St. Louis, MO). Humic acid was purchased from Tianjin Guangfu Fine Chemical Research Institute (Tianjin, China), formic acid was purchased from Tianjin Kermel Chemical Reagent Co., Ltd (Tianjin, China), and methanol was purchased from Xilong Chemical Engineering Co., Ltd (Guangdong, China). The solutions were prepared with ultrapure water, and all equipment used was washed with ultrapure water at 105 °C for 24 h before use. Hydrogen peroxide (H_2O_2, 30 wt%, analytical reagent grade) was purchased from Sinopharm Chemical Reagents Co., Ltd (Shanghai, China).

UV/H_2O_2/O_3 system

Experiments were carried out at the pilot plant of the Quehua Water Plant in Jinan, China. The test device (Figure 1) included a UV reactor with a volume of 2.4 L, which contained an ultraviolet lamp with intensity of 420 μW/cm^2. The DCBQ solution was pressurized and transferred to the UV reactor by a centrifugal pump. The main pipeline was connected to a H_2O_2 solution feeding facility and an O_3 gas feeding facility. The H_2O_2 solution feeding facility contained H_2O_2 solution that was transferred to the main pipeline by a metering pump. The O_3 gas feeding facility contained O_2, which was used to convert a certain concentration of O_3 gas by an O_3 generator. The generated O_3 gas was then transferred to the main pipeline through a gas flow meter. A gas concentration detector was used to detect the O_3 concentration.

Because the experiments were conducted in a continuous flow system, the O_3 concentration in the UV reactor could be determined from the mass balance using the following equation:

$$D_{O_3} = \frac{Q_G \times C_{O_3}}{Q_L} \tag{1}$$

where D_{O_3} is the concentration of O_3 gas (mg/L), Q_G is the O_3 gas flow rate (L/min), CO_3 is the O_3 gas concentration detected by the O_3 concentration detector (g/m^3 or mg/L), and Q_L is the liquid flow rate in the main line (L/min).

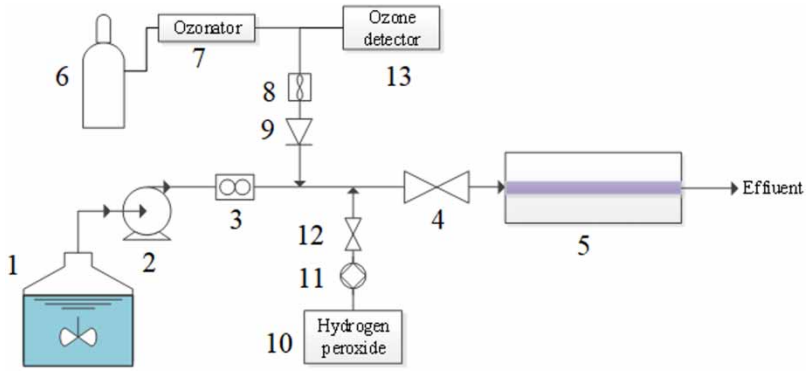

Figure 1 | 1. DCBQ solution tank; 2. Centrifugal pump; 3. Liquid rotor flowmeter; 4. Gate valve; 5. UV reactor (including UV lamp tube); 6. Oxygen tube; 7. O_3 generator; 8. Gas rotor flowmeter; 9. Check valve; 10. H_2O_2 solution tank; 11. Metering pump; 12. Gate valve; 13. O_3 gas concentration detector.

The concentration of H_2O_2 in the UV reactor was determined using the following equation:

$$D_{H_2O_2} = \frac{Q_{H_2O_2} \times C_{H_2O_2}}{Q_L} \quad (2)$$

where $D_{H_2O_2}$ is the concentration of H_2O_2 in the reactor (mg/L), $Q_{H_2O_2}$ is the metering pump flow rate (L/min), $C_{H_2O_2}$ is the H_2O_2 concentration in the H_2O_2 solution tank (mg/L), and Q_L is the liquid flow rate in the main line (L/min).

Before the experiments, the equipment was cleaned with purified water, which was removed before the test. A stock solution of DCBQ in methanol (50 mg/L) was diluted with water to prepare a DCBQ solution with a concentration of 1 μg/L. This solution was placed in the DCBQ solution tank. Next, a H_2O_2 solution was prepared and placed in the H_2O_2 solution tank. A centrifugal pump was used to control the liquid flow rate (Q_L) in the main circuit and adjust the residence time of the solution in the reactor. The O_3 and H_2O_2 concentrations in the gas flow meter and the metering pump control reactor were adjusted using Equations (1) and (2). Samples (500 mL) were collected at set intervals (1, 3, 5, and 7 min) for testing. Appropriate volumes of formic acid and 0.1 mol/L sodium thiosulfate aqueous solution were added for solid-phase extraction (SPE) on-machine detection.

Analytical method

The HBQ concentrations in the water samples after the advanced oxidation were determined by SPE ultra-performance liquid chromatography (UPLC) tandem MS. The detection limit of this method was 0.01 μg/L. The recoveries were 80.0–85.0%, and the relative standard error is 3.8–4.9%.

Sample preparation

Water samples were collected in brown bottles, and an appropriate volume of formic acid was added to adjust the pH to 2.6–2.8. Pretreatment by SPE was used to concentrate and enrich the target substances in the water samples. Before adding the sample solution, the Water Oasis HLB SPE column (Waters; Shanghai, China) was activated with a methanol solution containing 0.25% formic acid. And the column was washed twice with an aqueous solution containing 0.25% formic acid. During loading, each sample (500 mL) passed through the column at a flow rate of 8 mL/min. After loading the sample, the column was washed with an aqueous solution containing 0.25% formic acid and a solution containing methanol/water (50:50, v/v) containing 1% formic acid, and dried in vacuum for 10 min. The analyte from the extraction column is then eluted into a collection tube with a methanol solution containing 0.25% formic acid. The collected liquid was reduced dryness under a stream of nitrogen, and the residue was reconstituted in 1 mL of a water/methanol solution containing 0.25% formic acid (80:20, v/v) and placed in a sample bottle for analysis.

Detection method

Chromatography was performed with an Acquity UPLC BEH C18 analytical column (2.1 mm i.d., 50 mm long, 1.7 μm particle diameter, Waters, Shanghai, China). The mobile phase was a mixture of an aqueous 0.25% formic acid solution (A) and

methanol 0.25% formic acid solution with a flow rate of 0.4 mL/min. A gradient elution was performed as follows: 0–1 min, 20% B; 1–12 min, increased from 20% to 90% B; 12–14 min, 90% B; reduced to 20% B within 0.01 min; and 14.01–18 min, 20% B. The sample volume was 10 μL.

The MS was performed using electrospray ionization, negative ion scanning, and multiple reaction monitoring with the following parameters: negative ionization voltage, −4,500 V; solvent removal temperature, 350 °C; curtain air pressure, 207 kPa; spray gas pressure, 345 kPa; and auxiliary heating air pressure, 345 kPa.

UPLC–MS was used to identify DCBQ degradation intermediates. The MS was operated in electron impact ionization mode with an ion source temperature of 350 °C. Data were acquired 5 min after injection, and the *m/z* scan range was 30–500. The carrier gas pressure was kept constant at 100 kPa. The ionization energy was 70 eV, the MS resolution was 60,000, and all other parameters are set to default values.

Test design

The BBD and Central Composite Design are the most commonly used designs in Design-Expert. Compared with the BBD, the Central Composite Design requires more experiments, takes longer, and is more expensive for establishing model equations (Ferreira *et al.* 2007). Therefore, we used the BBD to evaluate the effects of the UV dose, O_3 concentration, and H_2O_2 concentration on the DCBQ removal rate. The values of the independent variables are shown in Table 1.

The experimental data from the BBD were analyzed by the Response Surface Regression program to fit the following second-order polynomial model (Nam *et al.* 2017):

$$Y = \beta_0 + \sum_{i=1}^{k} \beta_i X_i + \sum_{i=1}^{k} \beta_{ii} X_i^2 + \sum_{i=1}^{k} \sum_{j=1}^{k} \beta_{ij} X_i X_j + \cdots e \tag{3}$$

where Y is the predicted response value, X_i and X_j are variables, β_0 is a constant; β_i is a coefficient (linear term) that determines the influence of parameter i in the response, β_{ij} is a cross product coefficient, β_{ii} is a quadratic coefficient that represents the effect of interaction between independent variables; and e is random error. The coefficients could be obtained through multiple regression analysis, and equations could be used to predict the response values.

RESULTS AND DISCUSSION

Removal of DCBQ using O_3, H_2O_2, and UV advanced oxidation processes

Advanced oxidation processes with O_3 (2 mg/L), H_2O_2 (2 mg/L), and UV (420 μW/cm^2) were investigated for DCBQ removal (average concentration of 1 μg/L) (Figure 2).

In all cases, the removal of DCBQ was not satisfactory, with removal rates of 57.9, 32.0, and 36.1% for the processes using O_3, H_2O_2, and UV, respectively. Generally, O_3 attacks organic pollutants through two different mechanisms (Shen & Ku 1998): (1) direct oxidation of O_3 molecules and (2) indirect oxidation of highly reactive free radicals ($HO^{\cdot}$). Under acidic conditions, the direct oxidation of O_3 molecules predominates, the oxidation is weak, and the reaction has high selectivity (Yan 2019). An increase in pH will promote the decomposition of O_3 to $HO^{\cdot}$, as shown in Equation (4). Therefore, under alkaline conditions, free radical reactions may be dominant. The standard oxidation potential of $HO^{\cdot}$ is higher than that of O_3, and indirect oxidation with $HO^{\cdot}$ is more efficient than direct oxidation for the removal of DCBQ. Because the experiments were performed

Table 1 | Factors and levels

Factor	Coded identification	Level		
		−1	0	+1
UV dose (mJ/cm^2)	A	0	100	200
O_3 concentration (mg/L)	B	0	1	2
H_2O_2 concentration (mg/L)	C	0	1	2

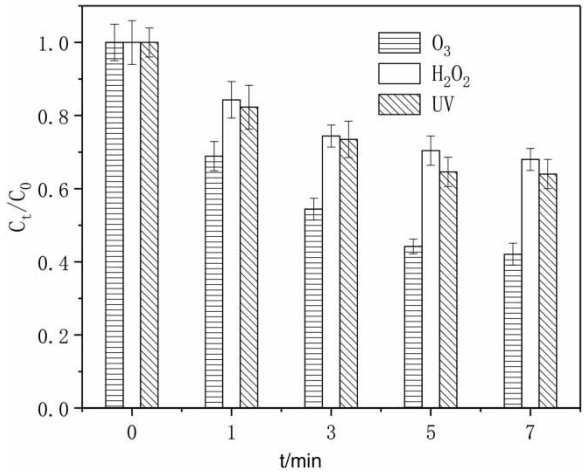

Figure 2 | O_3, H_2O_2, and UV technology comparison of DCBQ removal effect ([O_3] = 2 mg/L, [H_2O_2] = 2 mg/L, and UV dose = 180 mJ/cm^2).

in an acidic solution, the main reaction was direct oxidation of O_3 molecules and the removal of DCBQ was not ideal.

$$2O_3 + OH^- \rightarrow OH^{\cdot} + O_2^- + 2O_2 \tag{4}$$

The effect of H_2O_2 oxidation alone on DCBQ was not ideal. Because H_2O_2 itself is not a strong oxidant, Baciogliu & Otker (2003) used a H_2O_2 solution with a maximum concentration of 100 mmol/L to treat wastewater for 1 h. No changes in the chemical oxygen demand or UV_{254} were observed during the experiment.

UV degradation of DCBQ occurs through direct and indirect photolysis. In direct photolysis, some degradation of DCBQ occurs under UV irradiation because of the instability of DCBQ to light. In this pathway, after the DCBQ molecule absorbs UV energy, electron transfer or transition (Naijun 2017) results in a change from the ground state to the excited state, which changes the chemical structure of DCBQ. In indirect photolysis (Equation (5)), $HO^{\cdot}$ ($E_0 = 2.80$ V) acts as a strong oxidant and e_{aq}^-($E_0 = -2.9$ V) as a strong reductant (Yan 2019).

$$H_2O \xrightarrow{hv} OH^{\cdot} + e_{aq}^- + H^{\cdot} + H_2 + H_2O_2 + H_3O^+ \tag{5}$$

Although DCBQ can be removed by $HO^{\cdot}$ in UV indirect photolysis, UV photolysis of water molecules cannot generate sufficient $HO^{\cdot}$ for this process (Yan 2019). Consequently, DCBQ removal by UV indirect photolysis is negligible. Therefore, DCBQ removal using UV radiation on its own can take a long time.

To overcome these deficiencies, we used a BBD to optimize the parameters of the UV/H_2O_2/O_3 process for DCBQ removal.

Test results

Experiments were carried out using a three-factor, three-level BBD, and 17 groups of experiments with five center points were performed, which made the mathematical model statistically consistent. The dosage of UV, H_2O_2, and O_3 in the test was determined according to the above test. The results are shown in Table 2.

Model establishment and verification

Design-Expert 10.0 software was used to mathematically model the response values and factors in Table 2, and the following second-order polynomial equation was obtained:

$$\begin{aligned} Y = {} & 84.32 + 14.622X_1 + 21.501X_2 + 12.268X_3 - 15.237X_1X_2 - 9.547X_1X_3 \\ & - 11.98X_2X_3 - 0.868X_1^2 - 10.401X_2^2 - 1.961X_3^2 \end{aligned} \tag{6}$$

Table 2 | Experimental design results

	Factor			
Test number	UV dose (mJ/cm^2)	O_3 concentration (mg/L)	H_2O_2 concentration (mg/L)	DCBQ removal rate (%)
1	200	1	2	94.65
2	100	1	1	85.31
3	0	1	2	90.27
4	100	2	0	89.4
5	100	0	2	78.49
6	0	0	1	16.33
7	0	2	1	94.76
8	100	2	2	92.57
9	100	1	1	80.46
10	100	1	1	87.49
11	200	0	1	81.82
12	0	1	0	49.24
13	100	1	1	84.73
14	200	1	0	91.81
15	100	0	0	27.38
16	100	1	1	83.62
17	200	2	1	99.3

where Y is the DCBQ removal rate (%), X_1 is the UV dose (mJ/cm^2), X_2 is the O_3 concentration (mg/L), and X_3 is the H_2O_2 concentration (mg/L).

The model was statistically evaluated using the determination coefficient (R^2) and analysis of variance results. The analysis of model variance is shown in Table 3. The P-value of ≤ 0.0001 was taken as highly significant, $P \leq 0.05$ as significant, and $P > 0.05$ as not significant.

Table 3 | Model ANOVA

Source	Sum of squares	d.f.	Mean square	*F*-value	*P*-value
Model	8,973.36	9	997.04	44.80	<0.0001
X_1 – UV dose	1,710.54	1	1,710.54	76.87	<0.0001
X_2 – O_3 concentration	3,698.43	1	3,698.43	166.2	<0.0001
X_3 – H_2O_2 concentration	1,204.18	1	1,204.18	54.11	0.0002
X_1X_2	928.73	1	928.73	41.73	0.0003
X_1X_3	364.62	1	364.62	16.38	0.0049
X_2X_3	574.56	1	574.56	25.82	0.0014
X_1^2	3.18	1	3.18	0.14	0.7168
X_2^2	455.50	1	455.50	20.47	0.0027
X_3^2	16.19	1	16.19	0.73	0.4219
Residual	155.77	7	22.25		
Missing item	129.19	3	43.06	6.48	0.0514
Pure error	26.59	4	6.65		
Total variation	9,129.14	16			

$R^2 = 0.9829$, adjustment $R^2 = 0.9610$.

The *F*-value of the model was 44.80 (i.e., >0.001) (Table 3) and indicated that the model was highly significant. The *P*-value of the model was <0.0001 and indicated that the total variance that the model could not explain because of errors was only 0.01%. Mismatch terms were used to test the adequacy of model fitting according to data changes in the model. The *P*-value of the mismatch term was greater than 0.05, indicating that the *F*-value of the mismatch term (6.48) was not statistically significant. In addition, the mismatch term was not significant, which indicated that there was a significant correlation between the variable and response value. The *P*-values of X_1, X_2, X_3, X_1X_2, X_1X_3, X_2X_3, and X_2^2 were all less than 0.05, indicating that these terms were significant in the model. The coefficient of determination (R^2) is the ratio of the sum of regression squares and the sum of total squares and can be used to evaluate model fitting. In our experiments, $R^2 = 0.9829$ showed that the model could fit 98.29% of the total variables, so the model could fit the test data well (Sahoo & Gupta 2012). The corrected R^2 (0.9610) also showed that the model had good fit. For R^2, an increase will be observed as the independent variable increases. By contrast, for the corrected R^2, an increase will only be observed as the independent variable that has a significant impact on the model increases; otherwise, the corrected R^2 will decrease. Therefore, a small difference between R^2 and the corrected R^2 indicates that the model has good fit.

The coefficient of variation (CV) is the ratio of the standard error of the model to the average value of the actual response. When the CV value is less than 10%, the model is considered repeatable (Biglarijoo *et al.* 2016). The AP (Adeq Precision) value represents the range of predicted response values and their associated errors. The CV value of the present model was 6.04% (i.e., <10%) and the AP value was 21.322 (i.e., >4), which indicated that the model had high applicability. The *F*-value indicates the importance of the influence of an independent variable on the model. In this case, the order of influence of the independent variables on the model was O_3 concentration > UV dose > H_2O_2 concentration (Table 3).

The relationship between the measured value and the model's predicted response is shown in Figure 3(a), and the residual distribution of the model is shown in Figure 3(b). This relationship was almost linear, which indicated that the model had good fit.

Response surface analysis

A three-dimensional response surface map and a two-dimensional contour map of the regression model were obtained by fixing one variable and changing the other two variables. The interaction of various factors affected the curvature of the response surface map and the contour map. Figure 4 shows the response surface and contour plots of the effects of various factors on the DCBQ removal rate.

As the O_3 concentration and UV dose increased, the response surface graph and the contour map darkened (Figure 4(a1) and 4(a2)), indicating that the DCBQ removal rate increased. These results reflected the interaction between the UV dose (A) and O_3 concentration (B). When the H_2O_2 concentration was fixed (1 mg/L), no O_3 was added, and the UV dose was 100

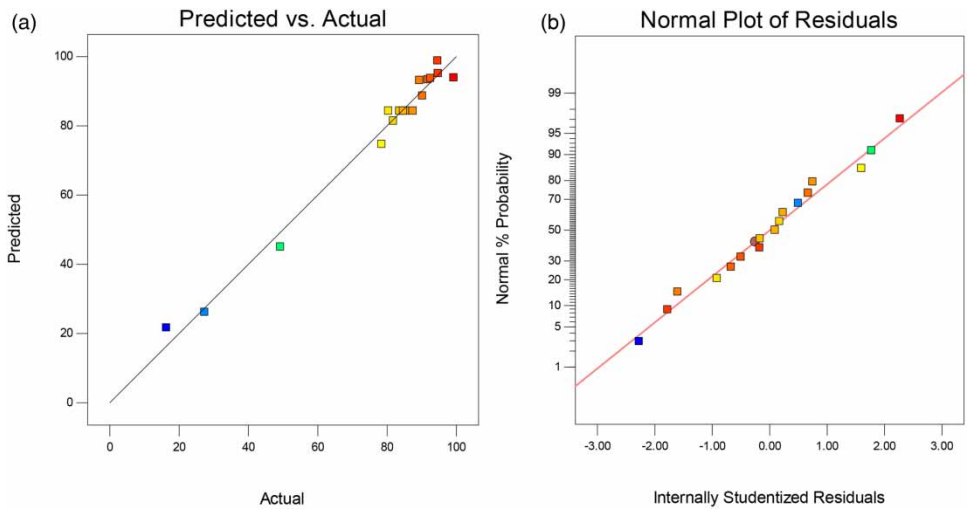

Figure 3 | Model fitting effect ((a) comparison of the actual value of response surface and response value and (b) residual distribution of the model).

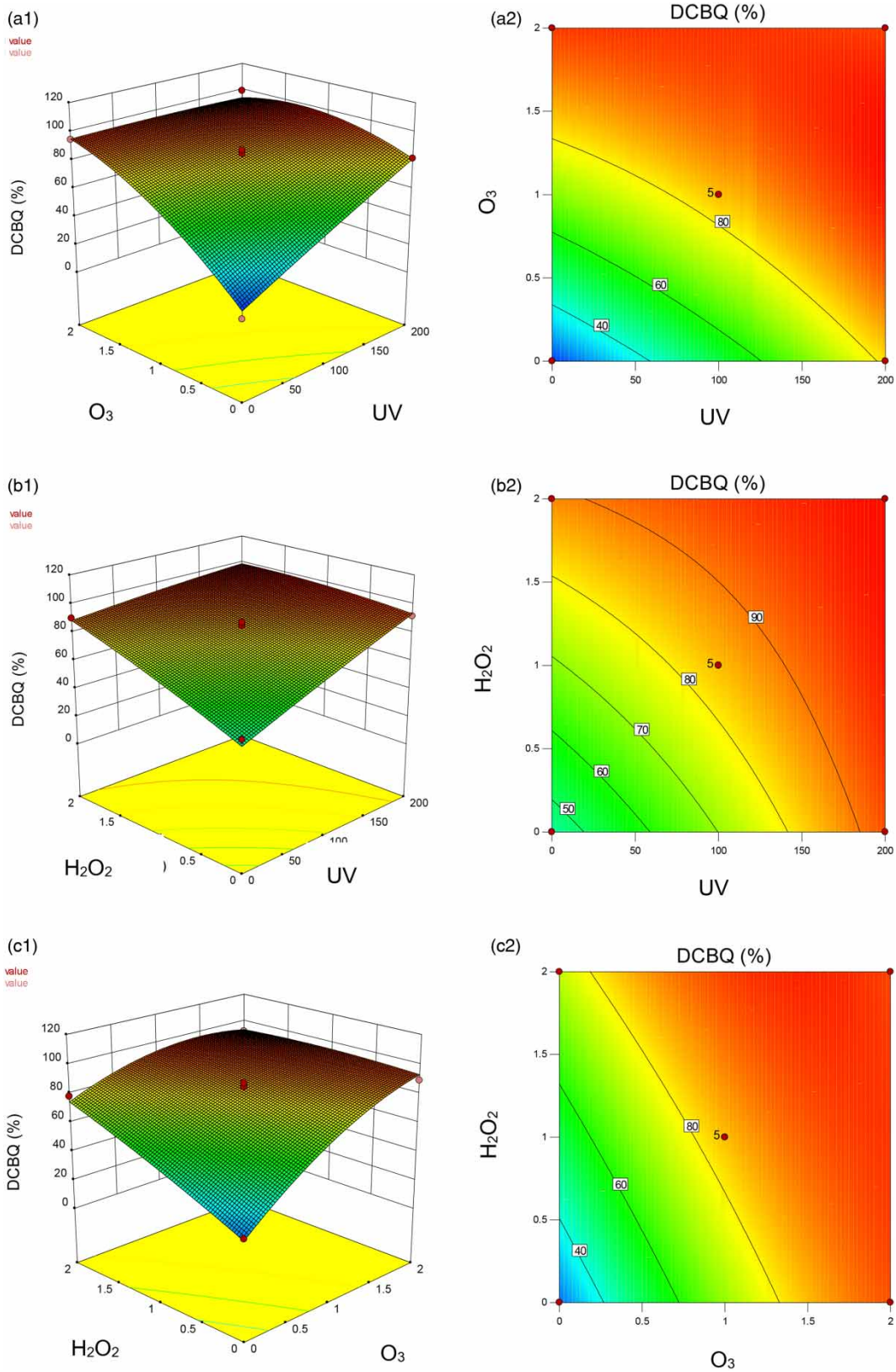

Figure 4 | Response surface and contour plots of the effects of various factors on the DCBQ removal rate (a1, a2, UV dose and O_3 concentration; b1, b2, UV dose and H_2O_2 concentration; c1, c2, O_3 concentration and H_2O_2 concentration).

mJ/cm^2, the DCBQ removal rate was only 52.5%. However, as the O_3 concentration increased, the DCBQ removal rate increased to 95.4%. In addition, when the O_3 concentration was fixed at 1 mg/L and the UV dose was increased from 0 to 200 mJ/cm^2, the DCBQ removal rate increased from 68.9 to 98.08%. When considering the DCBQ removal rate, the contribution of the O_3 concentration was more important than that of the UV dose.

When the O_3 concentration was fixed, as the UV dose and H_2O_2 concentrations increased, the response surface graph and contour map darkened and the DCBQ removal rate increased (Figure 4(b1) and 4(b2)). These results reflected the interaction between the UV dose (A) and H_2O_2 concentration (C) on the DCBQ removal rate. The changes observed showed that the order of importance of the variables for their influence on the DCBQ removal rate was UV dosage > H_2O_2 concentration.

When the UV dose was fixed, as the O_3 and H_2O_2 concentrations increased, the color of the response surface map and the contour map darkened. The DCBQ removal rate changed (Figure 4(c1) and 4(c2)). These results reflected the interaction of the O_3 concentration (B) and H_2O_2 concentration (C) on the DCBQ removal rate. The changes observed showed that the degree of influence of the variables DCBQ removal rate was in the order O_3 concentration > H_2O_2 concentration. Therefore, the order of influence of the three variables on the DCBQ removal rate was O_3 concentration > UV dose > H_2O_2 concentration.

Optimization of the working conditions

The numerical optimization function in Design-Expert 10.0 was used to optimize the conditions for DCBQ removal. The measured values were compared with predicted values from the model (Table 4). Under the optimum conditions, the actual DCBQ removal rate was 94.30% and the predicted DCBQ removal rate was 95.34%. The relative error between the measured value and the predicted value was 1.1%, which indicated that the model had good applicability and reliability. The model has a certain guiding significance for the treatment of actual water body by advanced oxidation processes (AOPs). The HO$^{\cdot}$ produced by UV/H_2O_2/O_3 has a good effect on the disinfection and sterilization of drinking water (Li 2013).

Effect of NOM on DCBQ removal

Research has shown (Jia 2019) that NOM in water will affect the efficiency of advanced oxidation. Humic acid (HA) is a typical type of NOM in wastewater and surface water; therefore, we studied the influence of HA as a representative NOM on DCBQ removal.

During the experiment, the initial concentration of DCBQ was 1 μg/L, the UV intensity was 420 μW/cm^2, the average concentration of H_2O_2 was 1.36 mg/L, and the average concentration of O_3 was 0.51 mg/L. The HA concentrations were set at 0, 1, 5, and 10 mg/L, and the solutions were sampled at 1, 3, 5, and 7 min. The influence of HA concentration on the removal of DCBQ is shown in Figure 5.

When the initial HA concentrations were 1, 5, and 10 mg/L, the DCBQ removal rates at 7 min were 95.9, 83.1, and 66.0%, respectively (Figure 5). The corresponding reaction rate constants were 0.46901, 0.28456, and 0.19617 min^{-1}. As the reaction time increased, the DCBQ removal rate increased, and the solution color lightened slightly. When the concentration of HA was 1 mg/L, it had a positive effect on DCBQ removal, while higher HA concentrations had an inhibitory effect. The promotion effect of HA at low concentration may be due to the obvious photosensitivity of HA at low concentrations (Verma *et al.* 2016), which means that HA can react with pollutants in water to form photooxidants and promote the reaction. In addition, there are many hydroxyl groups, phenolic hydroxyl groups, amino groups, and other functional groups distributed on the surface of HA, which can promote the decomposition of H_2O_2 to form HO$^{\cdot}$ under UV radiation (Aguer 1999). And the low concentration of HA may promote the decomposition of O_3 to produce HO$^{\cdot}$. Ultraviolet, ozone, and hydrogen peroxide react quickly to produce hydroxyl radicals. In the study of ozone decomposition rate in the UV/H_2O_2/O_3 oxidation system, Du (2020) found that the O_3 decay rate is extremely fast. Tan *et al.* (2013) obtained similar results in their experiments. Organic compounds have limited ability to consume ozone and hydrogen peroxide, but the high concentration of HA can

Table 4 | Verification of optimal working conditions

Factor					
UV dose (mJ/cm^2)	O_3 concentration (mg/L)	H_2O_2 concentration (mg/L)	Predicted removal rate	Actual removal rate	Error (%)
180	0.51	1.76	95.34	94.30	1.1

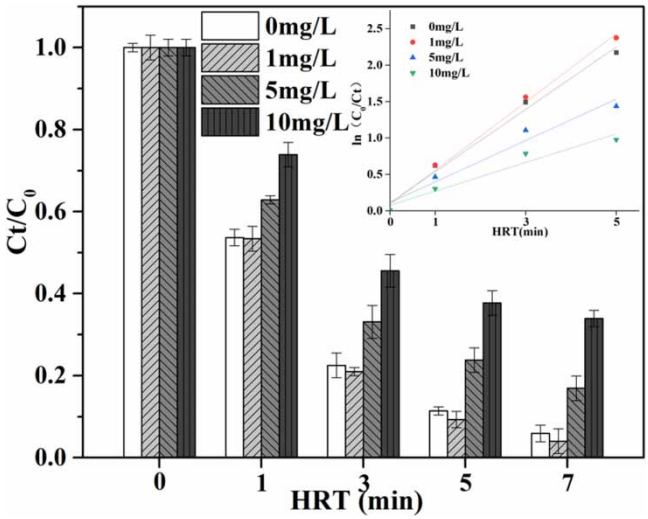

Figure 5 | Comparison of the removal effect of DCBQ with HA concentration.

compete with DCBQ to consume HO· and reduce the steady-state HO· concentration in solution (He *et al.* 2013). In addition, when HA concentration is high, the solution will turn brown and absorb photons, which will reduce the penetration rate of UV in the solution (Lutze & Bircher 2015). The reaction between NOM and HO·, which has a rate constant of $2.23 \times 10^8\ M^{-1}\ s^{-1}$, is shown in Equation (7).

$$NOM + HO^{\cdot} \rightarrow \text{Products} \tag{7}$$

CONCLUSIONS

DCBQ was removed from water using UV, H_2O_2, and O_3 advanced oxidation processes with removal rates of 36.1, 32.0, and 57.9%, respectively. These removal rates were not ideal, and these processes are not suitable for this application. Consequently, we used a BBD to optimize the operating parameters for the combined UV/H_2O_2/O_3 advanced oxidation process, and a quadratic model was established. The test data agreed well with the model and the correlation coefficient was greater than 0.98. The order of influence of the three factors for their effects on the DCBQ removal rate was O_3 concentration > UV dose > H_2O_2 concentration. The model we used had good applicability and reliability. We found that NOM in the water matrix affected the degradation of DCBQ in the UV/H_2O_2/O_3 process. When the concentration of HA was 1 mg/L, it had a positive effect on DCBQ removal, while higher HA concentrations inhibited DCBQ degradation.

ACKNOWLEDGEMENTS

The research was completed at the pilot scientific research base of the National Science and Technology Major Project of Jinan Water Supply and Drainage Monitoring Center under the Evaluation and Standardization of Key Technologies for Urban Water Supply System Operation Management project (2017ZX07501002). We thank the Shandong Province Water Supply and Drainage Monitoring Center for assistance with the experiments and valuable discussions.

DATA AVAILABILITY STATEMENT

All relevant data are included in the paper or its Supplementary Information.

REFERENCES

Aguer, J. P. R. C. A. F. 1999 Effect of light on humic substances: production of reactive species. *Analusis* **5** (27), 387–389.

Baciogliu, I. A. & Otker, M. 2003 Treatment of pharmaceutical wastewater containing antibiotics by O_3 and O_3/H_2O_2 processes. *Chemosphere* **50**, 85–95.

Biglarijoo, N., Mirbagheri, S. A., Ehteshami, M. & Ghaznavi, S. M. 2016 Optimization of Fenton process using response surface methodology and analytic hierarchy process for landfill leachate treatment. *Process Safety & Environmental Protection* **104**, 150–160.

Chen, L., Cai, T., Cheng, C., Xiong, Z. & Ding, D. 2018 Degradation of acetamiprid in UV/H_2O_2 and UV/persulfate systems: a comparative study. *Chemical Engineering Journal* **351**, 1137–1146.

Ding, C. S., Xiao, M., Zhao, S., Miao, S. & Zou, S. 2018 Performance of 2,6-DCBQ degradation in drinking water by potassium ferrate. *Journal of Zhejiang University of Technology* **46** (03), 337–341.

Du, Z. 2020 *Research on Degradation of Nitrosamine Precursor From Algae Organic Matter by UV/H_2O_2/O_3 Advanced Oxidation Technology*. Shandong Jianzhu University, Jinan, Shandong, China.

Du, Z., Jia, R., Li, C., Cui, P. & Liu, J. 2020 Pilot-scale UV/H_2O_2-BAC process for drinking water treatment – analysis and comparison of different activated carbon columns. *Chemical Engineering Journal* **382**, 123044.

Elibol, M. 2002 Response surface methodological approach for inclusion of perfluorocarbon in actinorhodin fermentation medium. *Process Biochemistry* **38** (5), 667–673.

Ferreira, S. L. C., Bruns, R. E., Ferreira, H. S., Matos, G. D., David, J. M., Brandao, G. C., da Silva, E. G. P., Portugal, L. A., dos Reis, P. S., Souza, A. S. & dos Santos, W. N. L. 2007 Box-Behnken design: an alternative for the optimization of analytical methods. *Analytica Chimica Acta* **597** (2), 179–186.

He, X., de la Cruz, A. A. & Dionysiou, D. D. 2013 Destruction of cyanobacterial toxin cylindrospermopsin by hydroxyl radicals and sulfate radicals using UV-254 nm activation of hydrogen peroxide, persulfate and peroxymonosulfate. *Journal of Photochemistry & Photobiology A Chemistry* **251**, 160–166.

Jia, H. Z. R. 2019 Elimination of trichloroanisoles by UV/H_2O_2: kinetics, degradation mechanism, water matrix effects and toxicity assessment. *Chemosphere* **230**, 258–267.

Li, Y. 2013 *Study on the Method of Emergency Drinking Water Disinfection Using Advanced Oxidation Technologies*. Dalian Maritime University. Dalian, Liaoning, China.

Lutze, H. V. & Bircher, S. 2015 Degradationof chlorotriazine pesticides by sulfate radicals and the influence of organic matter. *Environmental Science & Technology* **49** (3), 1673–1680.

Naijun, L. 2017 *Study on the Control Technology of Tetrachloro-P-Benzoquinone*. A Disinfection By-product in Drinking Water. Zhejiang University of Technology. Hangzhou, Zhejiang, China.

Nam, S. N., Cho, H., Han, J., Her, N. & Yoon, J. 2018 Photocatalytic degradation of acesulfame K: optimization using the Box-Behnken design (BBD). *Process Safety & Environmental Protection* **113**, 10–21.

Nikolaou, A. D., Lekkas, T. D. & Golfinopoulos, S. K. 2004 Kinetics of the formation and decomposition of chlorination by-products in surface waters. *Chemical Engineering Journal* **100** (1–3), 139–148.

Sahoo, C. & Gupta, A. K. 2012 Optimization of photocatalytic degradation of methyl blue using silver ion doped titanium dioxide by combination of experimental design and response surface approach. *Journal of Hazardous Materials* **215–216**, 302–310.

Schenone, A. V., Conte, L. O., Botta, M. A. & Alfano, O. M. 2015 Modeling and optimization of photo-Fenton degradation of 2,4-D using ferrioxalate complex and response surface methodology (RSM). *Journal of Environmental Management* **155**, 177–183.

Shen, Y. S. & Ku, Y. 1998 Decomposition of gas-phase chloroethenes by UV/O_3 process. *Water Research* **32** (9), 2679.

Shimabuku, K. K., Zearley, T. L., Dowdell, K. S. & Summers, R. S. 2019 Biodegradation and attenuation of MIB and 2,4-D in drinking water biologically active sand and activated carbon filters. *Environmental Science Water Research & Technology* **5** (5), 849–860.

Tan, C., Gao, N., Deng, Y., Zhang, Y., Sui, M., Deng, J. & Zhou, S. 2013 Degradation of antipyrine by UV, UV/H_2O_2 and UV/PS. *Journal of Hazardous Materials* **260**, 1008–1016.

Verma, S., Nakamura, S. & Sillanp, M. 2016 Application of UV-C LED activated PMS for the degradation of anatoxin-a. *Chemical Engineering Journal* **284**, 122–129.

Wang, W., Moe, B., Li, J., Qian, Y., Zheng, Q. & Li, X. 2016 Analytical characterization, occurrence, transformation, and removal of the emerging disinfection by products halobenzoquinones in water. *Trends in Analytical Chemistry* **85**, 97–110.

Yan, W. E. A. 2019 Degradation of clofibric acid by UV, O_3 and UV/O_3 processes: performance comparison and degradation pathways. *Journal of Hazardous Materials* **379** (5), 120771.

Zhao, Y., Qin, F., Boyd, J. M., Anichina, J. & Li, X. 2010 Characterization and determination of chloro- and bromo-benzoquinones as new chlorination disinfection byproducts in drinking water. *Analytical Chemistry* **82** (11), 4599–4605.

Zuo, Y., Hu, Y., Lu, W., Cao, J., Wang, F., Han, X., Lu, W. & Liu, A. 2017 Toxicity of 2,6-dichloro-1,4-benzoquinone and five regulated drinking water disinfection by-products for the Caenorhabditis elegans nematode. *Journal of Hazardous Materials* **321**, 456–463.

First received 30 January 2021; accepted in revised form 17 May 2021. Available online 2 August 2021